Available online at www.sciencedirect.com
SCIENCE DIRECT®
Journal of Organometallic Chemistry 690 (2005) 394–402
Journal of Organometallic Chemistry
www.elsevier.com/locate/jorganchem

Syntheses, crystal structures, and third-order nonlinear optical properties of two novel Mo/Cu/S clusters: $[MoS_4Cu_4(\alpha\text{-MePy})_5Br_2] \cdot 2(\alpha\text{-MePy})_{0.5}$ and $\{[MoS_4Cu_4(\alpha\text{-MePy})_3Br](\mu\text{-Br}) \cdot (\alpha\text{-MePy})\}_n$ (α-MePy = α-methylpyridine)

Wen-Hua Zhang [a], Jin-Xiang Chen [a], Hong-Xi Li [a], Bin Wu [a], Xiao-Yan Tang [a], Zhi-Gang Ren [a], Yong Zhang [a], Jian-Ping Lang [a,b,*], Zhen-Rong Sun [c]

[a] *Key Laboratory of Organic Synthesis of Jiangsu Province, School of Chemistry and Chemical Engineering, Suzhou University, Suzhou 215006, Jiangsu, PR China*
[b] *State Key Laboratory of Organometallic Chemistry, Shanghai Institute of Organic Chemistry, Chinese Academica of Sciences, Shanghai 200032, PR China*
[c] *Key Laboratory of Optical and Magnetic Resonance Spectroscopy, Department of Physics, East China Normal University, Shanghai 200062, PR China*

Received 15 June 2004; accepted 22 September 2004

This paper is dedicated to 70th birthday of Prof. Xin-Quan Xin at Nanjing University in China

Abstract

Reactions of $(NH_4)_2MoS_4$ with 4 equiv. of CuBr and 1 equiv. of AgBr in excess α-methylpyridine (α-MePy) gave rise to a pentanuclear cluster $[MoS_4Cu_4(\alpha\text{-MePy})_5Br_2] \cdot 2(\alpha\text{-MePy})_{0.5}$ (**1**) while those of $(NH_4)_2MoS_4$ with 4 equiv. of CuBr in α-MePy afforded a one-dimensional polymeric cluster $\{[MoS_4Cu_4(\alpha\text{-MePy})_3Br](\mu\text{-Br}) \cdot (\alpha\text{-MePy})\}_n$ (**2**). The X-ray analysis of **1** and **2** showed that the four copper atoms in **1** or **2** are coordinated by a central tetrahedral $[MoS_4]^{2-}$ ligand via four μ_3-S atoms, giving a MoS_4Cu_4 fragment with an approximate D_{2d} symmetry. Each fragment in **2** is further interconnected by a μ-Br atom to form a one-dimensional zig-zag chain. The nonlinear optical (NLO) property of **1** and **2** was studied by 35 ps laser pulses, and their third-order nonlinear susceptibility $\chi^{(3)}$ was measured by DFWM.

Keywords: Molybdenum cluster; Copper cluster; Crystal structures; Sulfide cluster; Non-linear optical properties

1. Introduction

Tetrathiometallate anions $[MS_4]^{2-}$ (M = Mo, W) and their clusters with various transition metals are well documented owing to their rich coordination chemistry [1–12], their relations to industrial catalysis process [13–15], biological systems [16–19], and photonic materials [20,21]. It is noteworthy that the Mo(W)/Cu(Ag)/S clusters, especially those containing pyridine and its derivatives, e.g. $[WS_4Cu_4I_2(Py)_6]$, have exhibited very good nonlinear optical properties in solution [22]. Those clusters have usually been prepared either from the reaction of $[MS_4]^{2-}$ with Cu^+ or Ag^+ under the presence of the basic ligands such as pyridine and its derivatives or

* Corresponding author. Tel.: +86 512 65213506; fax: +86 512 65224783.
E-mail address: jplang@suda.edu.cn (J.-P. Lang).

0022-328X/$ - see front matter © 2004 Elsevier B.V. All rights reserved.
doi:10.1016/j.jorganchem.2004.09.052

from the substitution of the labile ligands coordinated at metals of some preformed clusters with pyridine and its derivatives [23,24]. On the other hand, we have recently been interested in synthesis of Mo(W)/Cu(Ag)/S clusters from $[MS_4]^{2-}$ or $[Cp^*MS_3]^-$ (M = Mo, W) and their third-order nonlinear optical (NLO) properties [25,26]. As our continuing efforts to make new clusters for the NLO materials, we herein report the preparation, structural characterization and third-order NLO properties of two novel clusters $[MoS_4Cu_4(\alpha\text{-MePy})_5Br_2]\cdot 2(\alpha\text{-MePy})_{0.5}$ (**1**) and $\{[MoS_4Cu_4(\alpha\text{-MePy})_3Br](\mu\text{-Br})\cdot(\alpha\text{-MePy})\}_n$ (**2**), which were isolated from reactions of $(NH_4)_2[MoS_4]$ with CuBr/AgBr or CuBr in α-methylpyridine.

2. Results and discussion

2.1. Synthesis

Under the presence of basic ligands such as pyridine and its derivatives, copper(I) ion showed different reactivity toward $[MS_4]^{2-}$ relative to $Ag^+/[MS_4]^{2-}$ system. For instance, reactions of $(NH_4)_2[MS_4]$ with CuX in pyridine gave rise to a set of neutral pentanuclear bimetallic clusters $[MS_4Cu_4X_2(Py)_6]$ (M = Mo, W; X = Cl, Br, I, NCS) [22,23a], whereas those of $(NH_4)_2[MS_4]$ with AgX (X = Cl, Br, I) in pyridine and its derivatives formed a series of one-dimensional polymeric clusters $[RPyH]_n[MS_4Ag]_n$ (M = Mo, W, R = H, α-MePy, β-MePy, γ-MePy) [23b]. What will happen if the thiometallates react with Cu^+ and Ag^+ together in pyridine and its derivatives? With this question in mind, we carried out reactions of $(NH_4)_2[MoS_4]$ with 4 equiv. of CuBr and 1 equiv. of AgBr in excess α-MePy. A standard workup did not produce the expected trimetallic Mo/Cu/Ag/S cluster but a bimetallic pentanuclear cluster $[MoS_4Cu_4(\alpha\text{-MePy})_5Br_2]\cdot 2(\alpha\text{-MePy})_{0.5}$ (**1**) as red plates in 63% yield (Scheme 1). Reaction between $(NH_4)_2[MoS_4]$ with CuBr and AgBr in different molar ratios (1:3–4:1–2) always led to the formation of **1**. If the amount of AgBr used in the reaction was increased (e.g., $(NH_4)_2[MoS_4]$/CuBr/AgBr = 1:4:8 (molar ratio)), a large amount of crystals of $[\alpha\text{-MePyH}]_n[MoS_4Ag]_n$ coupled with a trace amount of crystals of **1** was isolated. However, the analogous reaction without AgBr generated a new polymeric cluster $\{[MoS_4Cu_4(\alpha\text{-MePy})_3Br](\mu\text{-Br})\cdot(\alpha\text{-MePy})\}_n$ (**2**) as red blocks in 82% yield. Since the formation of **1** apparently depends on the presence of AgBr relative to the formation of **2**, the role of AgBr deserves comment. AgBr may partly dissolve in α-MePy and react with $[MoS_4]^{2-}$ to form polymeric $[AgMoS_4]_n^{n-}$ species [23b,23e]. The presence of such chain-like species may prevent the formation of the polymeric W/Cu/S species like **2** in solution and thus promote the formation of the discrete molecule **1**. As discussed later in this paper, compound **1** is structurally related to other two Mo/Cu/S clusters $[MoS_4Cu_4Py_6Br_2]_n$ [23c] and $[PPh_4]_2[MoS_4(CuBr)_4]$ [5b]. However, their synthetic procedures are somewhat different. The latter two compounds were prepared either from substitution of part of bromides of the preformed cluster $[(n\text{-Bu})_4N]_4[MoS_4Cu_6Br_8]$ via pyridine or from reactions of $[PPh_4]_2[MoS_4]$ with CuBr in acetone.

Compounds **1** and **2** are relatively stable toward air and moisture. They are soluble in DMF and MeCN, and insoluble in Et_2O, MeOH, CH_2Cl_2 and $CHCl_3$. The elemental analysis of **1** or **2** is consistent with their chemical formula. The FT-IR spectra of **1** and **2** display Mo–S_{br} stretching vibration bands at 449/423 (**1**) and 443/415 (**2**) cm^{-1}. As shown in Fig. 1, the electronic spectrum of **1** or **2** exhibits a broad absorption bands at 521 (**1**) or 506 (**2**) nm, which is probably originated from sulfur to tungsten charge-transfer transition of the MoS_4 moiety [10]. The ^1H NMR spectra of **1** and **2** in DMSO-d_6 at ambient temperature display multiplets for the protons of α-MePy at 7.43–7.79 ppm (**1**) and 7.38–7.80 ppm (**2**) and a single resonance of CH_3 group at 3.33 (**1**) and 3.32 (**2**), respectively. Their similar

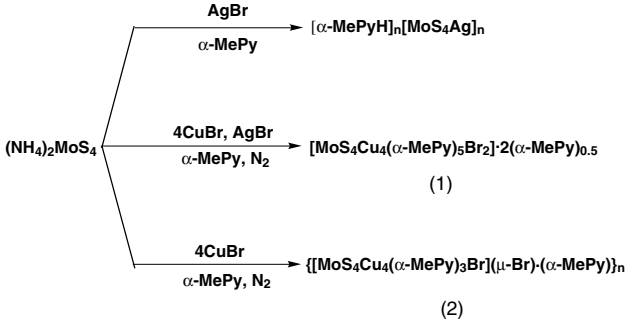

Scheme 1.

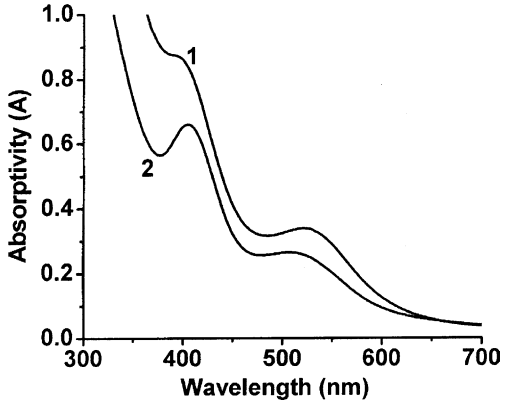

Fig. 1. Electronic spectra of **1** and **2** in DMF with concentrations of 1.5×10^{-4} M in a 1 cm thick glass cell.

^{1}H NMR patterns suggest that the solution structure of **2** may be different from its polymeric structure demonstrated by X-ray diffraction discussed below.

2.2. Crystal structure of $[MoS_4Cu_4(\alpha\text{-}MePy)_5Br_2]\cdot 2(\alpha\text{-}MePy)_{0.5}$ (**1**)

Crystal **1** crystallizes in the triclinic space group $P\bar{1}$ and an asymmetric unit contains an independent $[MoS_4Cu_4(\alpha\text{-}MePy)_5Br_2]$ molecule and two one-half of α-MePy solvated molecules. There is no evident interaction between the cluster and the α-MePy solvated molecules. Fig. 2 shows the perspective view of $[MoS_4Cu_4(\alpha\text{-}MePy)_5Br_2]$ molecule and Table 1 lists its selected bond lengths and angles. In the structure of $[MoS_4Cu_4(\alpha\text{-}MePy)_5Br_2]$ molecule, each of the four copper atoms is attached to one edge of the MoS_4 tetrahedron to form a saddle-like MoS_4Cu_4 structure with an approximate D_{2d} symmetry. The oxidation states for Mo and each of the four Cu atoms remain to be +6 and +1, respectively. The MoS_4Cu_4 skeleton of **1** closely resembles those observed in $[PPh_4]_2[MoS_4(CuBr)_4]\cdot Me_2CO$ [5b], $[A]_2[MS_4Cu_4(NCS)_4]^{2-}$ (A = PPh_4, NEt_4, M = Mo, W) [27a], $[NBu_4]_2[MoS_4(CuCl)_4]$ [27b], $[MS_4Cu_4Py_6X_2]$ (M = Mo, W; X = Cl, Br, I, SCN) [22], and $[MS_4Cu_4(dppm)_4](PF_6)_2$ (M = Mo, W) [25a]. Interestingly, compared with the reported symmetric structures $[MS_4Cu_4Py_6X_2]$, the structure of $[MoS_4Cu_4(\alpha\text{-}MePy)_5Br_2]$ of **1** is unsymmetric in that Cu(1) coordinates only one α-MePy while the other coppers coordinate either one α-MePy and one Br or two α-MePy molecules. Therefore Cu(1) assumes an approximate trigonal planar coordination geometry and Cu(2), Cu(3) and Cu(4) have a distorted tetrahedral geometry. Because of the different coordination geometries of copper atoms, the Mo···Cu contacts of **1** are different: one short Mo(1)···Cu(1) bond (2.629(3) Å) and three long Mo(1)···Cu bonds (2.669(3)–2.703(4) Å). The observed trend of Mo(1)···Cu contacts correlates with the number of bonding interactions at Cu centers. The short Mo(1)···Cu(1) contact occurs at Cu(1), which interacts with N (α-MePy), two μ_3-S and one Mo atom, and is comparable to those observed in clusters containing trigonally-coordinated Cu such as $[NBu_4]_2[MoS_4(CuCl)_4]$ (av. 2.609(2) Å) [27b], $[PPh_4]_2[(Cp^*MoS_3Cu_3Br_2)_2(\mu\text{-}Br)_2]$ (av. 2.652 Å) [28]. The long Mo(1)···Cu separations are observed for Cu(2), Cu(3) and Cu(4), which interact with two μ_3-S, two N (α-MePy) (or one N(α-MePy) and one Br) ligands and one Mo atom, and are close to those reported in $[MoS_4Cu_4Py_6I_2]$ (2.658(3)–2.697(3) Å) [23a], but shorter than those found in clusters containing tetrahedrally-coordinated Cu such as $[Cu_3MoS_3Br](PPh_3)_3S\cdot 0.5Me_2CO$ (2.776(2)–2.840(3) Å) [1b], and $[MoS_4Cu_4(dppm)_4](PF_6)_2$ (2.737(2)–2.747(2) Å) [25a]. The Cu-μ_3-S bond lengths also reflect the mode of coordination of the copper atoms: av. 2.275 Å for a trigonal geometry and av. 2.313 Å for a tetrahedral environment. The mean Cu–μ_3-S distance (2.304 Å) is similar to those reported in $[MoS_4Cu_4Py_6I_2]$ (av.

Table 1
Selected bond lengths (Å) and angles (°) for $[MoS_4Cu_4(\alpha\text{-}MePy)_5Br_2]\cdot 2(\alpha\text{-}MePy)_{0.5}$ (**1**)

Mo(1)···Cu(1)	2.629(3)	Mo(1)···Cu(2)	2.703(4)
Mo(1)···Cu(3)	2.690(3)	Mo(1)···Cu(4)	2.669(3)
Mo(1)–S(1)	2.264(6)	Mo(1)–S(2)	2.236(5)
Mo(1)–S(3)	2.251(5)	Mo(1)–S(4)	2.251(5)
Br(1)–Cu(2)	2.496(3)	Br(2)–Cu(4)	2.643(4)
Cu(1)–S(1)	2.283(6)	Cu(1)–S(4)	2.266(6)
Cu(1)–N(1)	1.99(1)	Cu(2)–S(1)	2.320(6)
Cu(2)–S(2)	2.320(6)	Cu(2)–N(2)	2.06(2)
Cu(3)–S(2)	2.316(5)	Cu(3)–S(3)	2.316(5)
Cu(3)–N(3)	2.10(2)	Cu(3)–N(4)	2.09(2)
Cu(4)–S(3)	2.292(5)	Cu(4)–S(4)	2.315(6)
Cu(4)–N(5)	2.04(2)	Cu(1)···Br(2)	2.991(4)
Cu(1)···Mo(1)···Cu(3)	172.54(12)	Cu(2)···Mo(1)···Cu(4)	169.05(11)
S(1)–Mo(1)–S(2)	109.5(2)	S(1)–Mo(1)–S(3)	110.7(2)
S(1)–Mo(1)–S(4)	108.9(2)	S(2)–Mo(1)–S(3)	110.2(2)
S(2)–Mo(1)–S(4)	108.4(2)	S(3)–Mo(1)–S(4)	109.2(2)
S(1)–Cu(1)–S(4)	107.7(2)	S(1)–Cu(1)–N(1)	125.1(5)
S(4)–Cu(1)–N(1)	123.0(5)	N(1)–Cu(1)–Mo(1)	169.4(5)
S(1)–Cu(2)–S(2)	104.8(2)	S(1)–Cu(2)–N(2)	115.6(5)
S(1)–Cu(2)–Br(1)	113.3(2)	S(2)–Cu(2)–N(2)	111.1(5)
S(2)–Cu(2)–Br(1)	105.5(2)	N(2)–Cu(2)–Br(1)	106.2(5)
S(2)–Cu(3)–S(3)	105.2(2)	S(2)–Cu(3)–N(3)	113.7(6)
S(2)–Cu(3)–N(4)	106.6(5)	S(3)–Cu(3)–N(3)	108.2(5)
S(3)–Cu(3)–N(4)	116.7(5)	N(3)–Cu(3)–N(4)	106.6(7)
S(3)–Cu(4)–S(4)	105.6(2)	S(3)–Cu(4)–N(5)	131.7(5)
S(3)–Cu(4)–Br(2)	102.0(2)	S(4)–Cu(4)–N(5)	110.2(5)
S(4)–Cu(4)–Br(2)	96.8(2)	N(5)–Cu(4)–Br(2)	104.9(5)
Cu(1)–S(1)–Mo(1)	70.6(2)	Cu(1)–S(1)–Cu(2)	111.3(2)
Cu(2)–S(1)–Mo(1)	72.3(2)	Cu(2)–S(2)–Mo(1)	72.7(2)
Cu(2)–S(2)–Cu(3)	119.7(2)	Cu(3)–S(2)–Mo(1)	72.4(2)
Cu(3)–S(3)–Mo(1)	72.1(2)	Cu(3)–S(3)–Cu(4)	117.9(2)
Cu(4)–S(3)–Mo(1)	71.9(2)	Cu(1)–S(4)–Mo(1)	71.2(2)
Cu(1)–S(4)–Cu(4)	93.5(2)	Cu(4)–S(4)–Mo(1)	71.5(2)

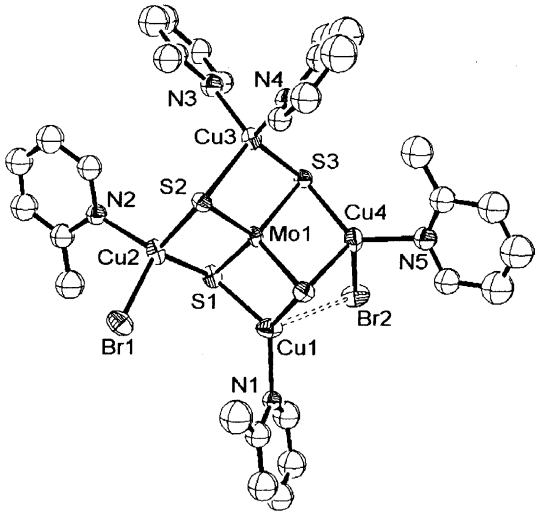

Fig. 2. Perspective view of the molecular structure of **1** with 50% thermal ellipsoids. All hydrogen atoms and solvent molecules are omitted for clarity.

2.286 Å) [23a] and $[PPh_4]_2[(Cp^*MoS_3Cu_3Br_2)_2(\mu\text{-}Br)_2]$ (2.234 Å) [28]. The Mo atom in the MoS_4Cu_4 core of **1** is at the centre of a slightly distorted tetrahedral MoS_4 unit being S–Mo–S angles of 108.4(2)–110.7(2)°. The mean Mo–μ_3-S bond length of 2.251 Å is slightly longer than that of $[MoS_4Cu_4(Py)_6I_2]$ (2.232 Å) [23a] and $[NBu_4]_2[MoS_4(CuCl)_4]$ (av. 2.230 Å) [27b]. We noticed a weak interaction between Cu(1) and Br(2) (2.991(4) Å), which may cause the Cu(4)–Br(2) bond distance (2.643 Å) to be longer than that of Cu(2)–Br(1) bond (2.496(3) Å). The average Cu–Br length of **1** (2.570 Å) is longer than that of the corresponding ones of $[PPh_4][Cp^*WS_3Cu_3Br_3(dppm)]$ (2.452 Å) [28]. The average Cu–N distance of 2.06 Å is comparable to those found in $[MoS_4Cu_4Py_6I_2]$ (av. 2.033 Å) [23a] and $[MoS_4Cu_6Py_4(\mu\text{-}Br)_2]_n$ (av. 1.970 Å) [23c].

2.3. Crystal structure of $\{[MoS_4Cu_4(\alpha\text{-}MePy)_3Br]\text{-}(\mu\text{-}Br)\cdot(\alpha\text{-}MePy)\}_n$ (2)

Crystal **2** crystallizes in the orthorhombic space group $Pca2_1$ and the an asymmetric unit contains one $[MoS_4Cu_4(\alpha\text{-}MePy)_3Br_2]$ molecule and one α-MePy solvated molecule. An X-ray analysis of **2** shows that it has a one-dimensional polymeric chain with the α-MePy solvated molecule inserted between chains (Fig. 3). There is no evident interaction between chains and between chains and the α-MePy solvent molecules. Table 2 presents the selected bond lengths and angles of **2**. As shown in Fig. 4, the repeating unit, $[MoS_4Cu_4(\alpha\text{-}MePy)_3Br_2]$, having the similar MoS_4Cu_4 skeleton of **2**, interconnects via μ-Br bridges into an infinite chain along *b* axis. Within the repeating unit, the four copper atoms have two different coordination geometries. Cu(1) and Cu(3) display a trigonal planar coordination geometry while Cu(2) and Cu(4) adopt a distort tetrahedral coordination geometry. Because of the different coordination geometry of the Cu atoms, the Mo···Cu contacts of **2** are also different: two short Mo(1)···Cu (2.6120(10)–2.6241(10) Å) and two long Mo(1)···Cu bonds (2.663(2)–2.676(2) Å). The observed trend of Mo(1)···Cu contacts correlates with the number of bonding interactions at Cu centers. The short Mo(1)···Cu contact occurs at Cu(1) and Cu(3), which interacts with two μ_3-S, one N(α-MePy) (or one Br) ligands and one Mo atom, while the long Mo(1)···Cu contacts are observed for Cu(2) and Cu(4), which interact with two μ-S, one N(α-MePy), one -Br and one Mo atom. The short and long Mo(1)···Cu contacts are comparable to those of the corresponding ones of **1**. The Cu–μ_3-S bond lengths also reflect the mode of coordination of copper atoms: av. 2.236 Å for a trigonal geometry and av. 2.293 Å for a tetrahedral environment. The mean Cu–μ_3-S distance (2.265 Å) is shorter than that of **1**. The mean Cu–μ-Br bond length

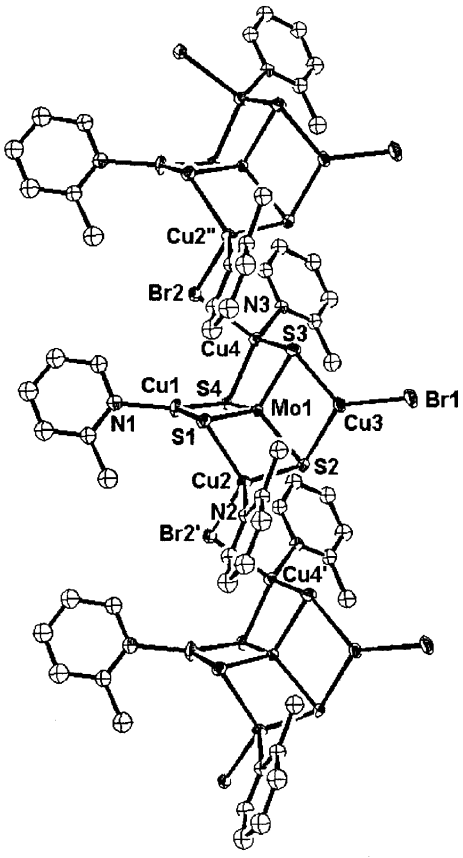

Fig. 3. Perspective view of a section of the 1D chain of **2** with 50% thermal ellipsoids. All hydrogen atoms and solvent molecules are omitted for clarity.

of 2.573 Å is similar to that in $[MoS_4Cu_6Py_4(\mu\text{-}Br)_2]_n$ (av. 2.587 Å) [23c], but longer than those observed in $[Cp^*WS_3Cu_2Br(\mu\text{-}Br)(PPh_3)_2]$ (2.640 Å) [29a], $[Et_4N]_2[Cu_2Br_4]$ (2.448 Å) [29b], and $[Pr_4^nN]_4[Cu_4Br_6]$ (2.398 Å) [29c]. The terminal Cu(3)–Br(1) length (2.2783(12) Å) is close to that of the corresponding one $[Cp^*WS_3Cu_2\text{-}Br(\mu\text{-}Br)(PPh_3)_2]$ (2.286(3) Å) [29a]. The mean Mo–μ_3-S length (2.243 Å) and Cu–N length (1.972 Å) are normal relative to those of the corresponding ones of **1**.

2.4. Non-linear optical (NLO) properties of 1 and 2

As shown in Fig. 1, both **1** and **2** have low absorbance at 532 nm. This promises low intensity loss and small temperature changes by photon absorption when the laser pulses propagate in the two materials. Results from DFWM are given in Figs. 5 and 6, in which the solid line is the theoretical fitted curve. The measured signal may originate not only from the nonlinear process of the ground states but also from the excited states and two-photon absorption and higher order optical nonlinearities for the high incident laser power. Under incident intensity of 0.2 mJ, the third-order susceptibility

Table 2
Selected bond lengths (Å) and angles (°) for $[MoS_4Cu_4(\alpha\text{-MePy})_3Br](\mu\text{-Br})\cdot(\alpha\text{-MePy})_n$ (**2**)

Mo(1)···Cu(1)	2.6120(10)	Mo(1)···Cu(2)	2.663(2)
Mo(1)···Cu(3)	2.6241(10)	Mo(1)···Cu(4)	2.676(2)
Mo(1)–S(1)	2.239(3)	Mo(1)–S(2)	2.247(2)
Mo(1)–S(3)	2.239(2)	Mo(1)–S(4)	2.246(3)
Br(1)–Cu(3)	2.2783(12)	Br(2)–Cu(4)	2.573(2)
Cu(1)–S(1)	2.255(3)	Cu(1)–S(4)	2.209(3)
Cu(1)–N(1)	1.934(6)	Cu(2)–S(1)	2.295(3)
Cu(2)–S(2)	2.289(3)	Cu(2)–N(2)	2.006(8)
Cu(3)–S(2)	2.243(3)	Cu(3)–S(3)	2.238(2)
Cu(4)–S(3)	2.301(3)	Cu(4)–S(4)	2.285(3)
Cu(4)–N(3)	1.975(8)		
Cu(1)···Mo(1)···Cu(3)	174.77(5)	Cu(2)···Mo(1)···Cu(4)	170.69(5)
S(1)–Mo(1)–S(2)	109.12(11)	S(1)–Mo(1)–S(3)	109.67(11)
S(1)–Mo(1)–S(4)	108.02(10)	S(2)–Mo(1)–S(3)	108.25(8)
S(2)–Mo(1)–S(4)	112.69(11)	S(3)–Mo(1)–S(4)	109.07(10)
S(1)–Cu(1)–S(4)	108.78(10)	S(1)–Cu(1)–N(1)	121.7(3)
S(4)–Cu(1)–N(1)	129.5(3)	S(1)–Cu(2)–S(2)	105.74(10)
S(1)–Cu(2)–N(2)	112.1(3)	S(2)–Cu(2)–N(2)	124.5(2)
S(2)–Cu(3)–S(3)	108.43(9)	S(2)–Cu(3)–Br(1)	127.08(8)
S(3)–Cu(3)–Br(1)	124.47(8)	S(3)–Cu(4)–S(4)	105.58(10)
S(3)–Cu(4)–N(3)	121.5(2)	S(3)–Cu(4)–Br(2)	99.06(9)
S(4)–Cu(4)–N(3)	116.1(3)	S(4)–Cu(4)–Br(2)	106.11(9)
N(3)–Cu(4)–Br(2)	106.2(2)	Cu(1)–S(1)–Mo(1)	71.06(9)
Cu(1)–S(1)–Cu(2)	108.87(12)	Cu(2)–S(1)–Mo(1)	71.91(9)
Cu(2)–S(2)–Mo(1)	71.88(8)	Cu(2)–S(2)–Cu(3)	118.02(13)
Cu(3)–S(2)–Mo(1)	71.53(7)	Cu(3)–S(3)–Mo(1)	71.78(7)
Cu(3)–S(3)–Cu(4)	118.37(12)	Cu(4)–S(3)–Mo(1)	72.22(8)
Cu(1)–S(4)–Mo(1)	71.79(9)	Cu(1)–S(4)–Cu(4)	100.46(12)
Cu(4)–S(4)–Mo(1)	72.39(9)		

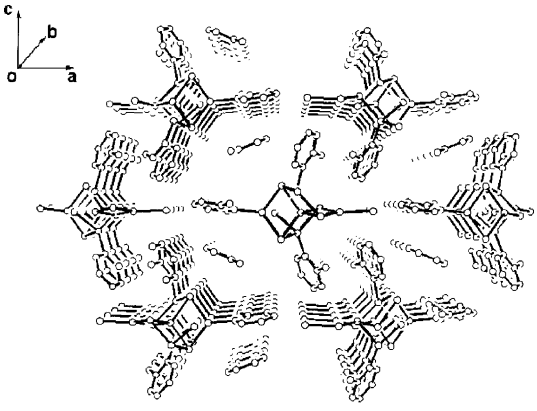

Fig. 4. Extended structure of **2** looking down the *b* axis.

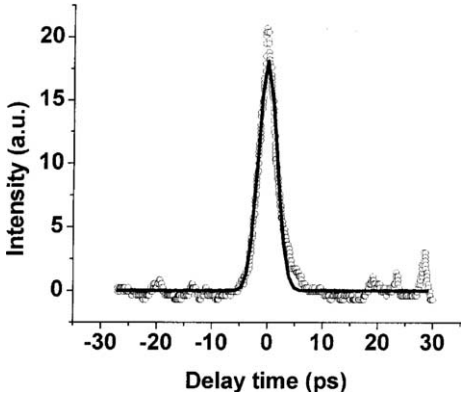

Fig. 5. The DFWM signal for **1** at 1.0×10^{-3} M in DMF with 35 ps laser and 1 mm cell.

$\chi^{(3)}$ (derived from Eq. (1)) and the second hyperpolarizability γ (derived from Eq. (2)) are obtained as 2.05×10^{-13} esu, 1.06×10^{-31} esu (**1**), and 2.01×10^{-13}, 1.02×10^{-31} esu (**2**), respectively. It is noted that most of the well performing third-order NLO materials reported in the literature are solid compounds such as metal polyyne polymers [30,31], metallophthalcyanine films [32,33], etc., which are neat materials. According to Eq. (2), N is the number density of a compound (concentration) and L_c is the Lorentz field factor correction. Therefore, we can use the hyperpolarizability γ to represent NLO properties of neat materials. Table 3 lists the γ value of some Mo(W)/Cu(Ag)/S clusters and known NLO materials for comparison. The γ values of **1** and **2** are comparable to those of the metal sulfide clusters derived from $[MS_4]^{2-}$ or $[MOS_3]^{2-}$ (M = Mo, W) and somewhat larger than those of C_{60} and C_{70} [34], organometallic compounds, and their films like TiOPc [30–33,35–37]. Considering the fact that the impressive γ values for **1** and **2** and other Mo(W)/Cu(Ag)/S clusters are obtained

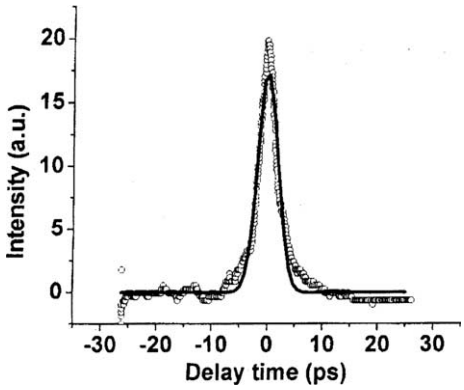

Fig. 6. The DFWM signal for **2** at 1.0×10^{-3} M in DMF with 35 ps laser and 1 mm cell.

from a very diluted solution, much better NLO performance can be anticipated if the solubility of the cluster can be improved significantly or a thin film of the cluster can be engineered.

3. Conclusions

We have demonstrated the preparation of two novel Mo/Cu/S clusters **1** and **2** from $(NH_4)_2MoS_4$/CuBr/AgBr/α-MePy or $(NH_4)_2MoS_4$/CuBr/α-MePy system. The molecular structures of **1** and **2** have been characterized by spectroscopy and X-ray analysis. Compound **1** or **2** consists of a MoS_4Cu_4 fragment with an approximate D_{2d} symmetry. In the structure of **2**, the μ-Br atom bound at one copper of the MoS_4Cu_4 fragment further links the other copper atom of another fragment to form a 1D zig-zag chain. Compounds **1** and **2** exhibit good NLO performance in solution. Therefore, they may be optimized for the photonic devices and may have potential applications in optical switches and OL materials.

4. Experimental

4.1. General

All manipulations were carried out under pure nitrogen using standard Schlenk techniques. $(NH_4)_2MoS_4$ was prepared according to the literature method [38]. Other chemicals were obtained from commercial sources and used as received. All solvents were predried over activated molecular sieves and refluxed over the appropriate drying agents under argon. The IR spectrum was recorded on a Nicolet MagNa-IR FT-IR spectrometer as KBr disk (4000–400 cm^{-1}). UV–Vis spectra were measured on a TU-1800SPC spectrophotometer. The elemental analysis for C, H, N were performed on a Carlo–Erba microanalyzer. ^1H NMR spectra were recorded at ambient temperature on a Varian UNITYplus-400 spectrometer. ^1H NMR chemical shifts were referenced to the DMSO-d_6 signal.

Table 3
Comparison of the γ value of some Mo(W)/Cu(Ag)/S clusters and known NLO materials

Compounds	γ (esu)	λ (nm)	Reference
$[(n\text{-}Bu)_4N]_2[MoOS_3(CuNCS)_3]$	4.8×10^{-29}	532	[20c]
$[MoOS_3Cu_3(4\text{-}pic)_6] \cdot 0.5[Mo_2O_7]$	1.32×10^{-30}	532	[22b]
$[WOS_3Cu_3(4\text{-}pic)_6] \cdot 0.5[Mo_2O_7]$	1.87×10^{-30}	532	[22b]
$[MoOS_3Cu_3(4\text{-}pic)_6](BF_4)$	2.89×10^{-31}	532	[22b]
$[WOS_3Cu_3(4\text{-}pic)_6](BF_4)$	4.43×10^{-31}	532	[22b]
$[MoS_4Cu_4(\alpha\text{-}MePy)_5Br_2] \cdot 2(\alpha\text{-}MePy)_{0.5}$	1.06×10^{-31}	532	This work
$\{[MoS_4Cu_4(\alpha\text{-}MePy)_3Br](\mu\text{-}Br) \cdot (\alpha\text{-}MePy)\}_n$	1.02×10^{-31}	532	This work
C_{60}	7.5×10^{-34}	1910	[34]
C_{70}	1.3×10^{-33}	1910	[34]
trans-$[Mo(CO)_4(PPh_3)_2]$	8.49×10^{-32}	532	[35]
cis-$[Mo(CO)_4(PPh_3)_2]$	4.375×10^{-31}	532	[35]
$[(\eta^5\text{-}C_5H_5)_2Ti(CCC_6H_5)_2]$	9.2×10^{-33}	1907	[36]
Platinum polyynes	5.6×10^{-35} ~8.56×10^{-34}	1064	[30,31]
Substituted benzoporphyrin zinc complexes	1.8×10^{-30} ~2.6×10^{-29}	532	[37]
H_2PcBu_4 (Pc = phthalocyanine)	~3×10^{-34}	1907	[32][a]
$VOPcBu_4$	~8×10^{-34}	1907	[32][b]
TiOPc	1.04×10^{-33}	1907	[33][c]
TiOPc	5.35×10^{-34}	1907	[33][d]

[a] 100% Pc film.
[b] PMMA doped film.
[c] Film before thermal annealing.
[d] Film after thermal annealing.

4.2. Synthesis

4.2.1. Preparation of $[MoS_4Cu_4(\alpha\text{-MePy})_5Br_2]\cdot 2(\alpha\text{-MePy})_{0.5}$ (1)

To a red solution of $(NH_4)_2MoS_4$ (0.026 g 0.1 mmol) in 15 mL of α-MePy was added CuBr (0.058 g 0.4 mmol) and AgBr (0.020 g 0.1 mmol). The mixture was stirred at ambient temperature for 40 min to give rise to dark red solution along with some insoluble solid, which was filtered off. Diethyl ether (20 mL) was slowly diffused into the filtrate to form red plates of $[MoS_4Cu_4(\alpha\text{-MePy})_5Br_2]\cdot 2(\alpha\text{-MePy})_{0.5}$ (**1**) one day later, which were collected by filtration, washed with MeCN and Et_2O, and dried in vacuo. Yield: 0.082 g (67%). Anal. Calc. for $C_{36}H_{42}Br_2Cu_4MoN_6S_4$: C 36.12, H 3.54, N 7.02. Found: C 36.45, H 3.59, N 7.33. UV–Vis (DMF, λ_{max}/nm (ε/$M^{-1}cm^{-1}$)): 521 (2300), 393 (5900). IR (cm^{-1}): 3055 (w), 1606 (s), 1486 (s), 1453 (s), 1382 (w), 1302 (s), 1154 (w), 1107 (m), 1063 (m), 1028 (w), 802 (w), 773 (s), 765 (s), 722 (w), 493 (m), 449 (m), 423 (w). ^1H NMR (DMSO-d_6, 400 MHz, 25 °C): δ 7.43–7.79 (m, 20H, Py), 3.33 (s, 15H, CH_3).

4.2.2. Preparation of $\{[MoS_4Cu_4(\alpha\text{-MePy})_3Br](\mu\text{-Br})\cdot(\alpha\text{-MePy})\}_n$ (2)

To a red solution of $(NH_4)_2MoS_4$ (0.026 g 0.1 mmol) in 15 mL of α-MePy was added CuBr (0.058 g 0.4 mmol). The mixture was allowed to stir at ambient temperature for 40 min to afford a homogeneous solution. Diethyl ether (20 mL) was slowly diffused into the solution to form red block crystals of $\{[MoS_4Cu_4(\alpha\text{-MePy})_3Br](\mu\text{-Br})\cdot(\alpha\text{-MePy})\}_n$ (**2**) three days later, which were collected by filtration, washed with MeCN and Et_2O, and dried in vacuo. Yield: 0.083 g (82%). Anal. Calc. for $C_{24}H_{28}Br_2Cu_4MoN_4S_4$: C 28.52, H 2.79, N 5.54. Found: C 28.50, H 2.83, N 5.54. UV–Vis (DMF, λ_{max}/nm (ε/$M^{-1}cm^{-1}$)): 506 (1800), 404 (4400). IR (cm^{-1}): 3444 (m), 3048 (w), 3032 (w), 2914 (w), 1606 (s), 1565 (w), 1487 (vs), 1453 (s), 1383 (w), 1302 (s), 1158 (m), 1062 (m), 763 (s), 722 (m), 492 (w), 443 (m), 415 (w). ^1H NMR (DMSO-d_6, 400 MHz, 25 °C): δ 7.38–7.78 (m, 12H, Py), 3.32 (s, 9H, CH_3).

4.2.3. X-ray crystallography

Diffraction data for **1** and **2** were collected on a Rigaku Mercury CCD X-ray diffractometer employing graphite-monochromated Mo Kα radiation (λ = 0.71070 Å). A red plate crystal of **1** with dimensions $0.45\times0.35\times0.15$ mm and a red block crystal of **2** with dimensions $0.45\times0.40\times0.12$ mm were mounted on glass fibers, and cooled at 193 K in a liquid nitrogen stream. Diffraction data were collected at ω mode with a detector to crystal distance of 35 mm. Indexing was performed from 6 images each of which was exposed for 15 s. Cell parameters were refined by using the program CrystalClear (Rigaku and MSC, Ver. 1.30, 2001) on all observed reflections between θ of 3.0° and 27.5°. A total of 1080 (**1**) and 1440 (**2**) oscillation images were collected in the range $1.92° < 2\theta < 54.96°$ (**1**) and $1.99° < 2\theta < 54.96°$ (**2**), respectively. The collected data were reduced by using the program CrystalStructure (Rigaku and MSC, Ver 3.60, 2004), and an absorption correction (Multi-Scan) was applied which resulted in transmission factors ranging from 0.300 to 0.572 (**1**) and from 0.178 to 508 (**2**). The reflection data were also corrected for Lorentz and polarization effects.

The crystal structures of **1** and **2** were solved by heavy-atom Patterson methods (**1**) [39] and Direct methods (**2**) [40], and expanded using Fourier techniques [41]. For **1** and **2**, all non-hydrogen atoms except those of α-MePy molecules were refined anisotropically. Due to the slow evaporization of the solvated α-MePy molecules in crystal **1**, two of them were fixed with constrained parameters and refined with an occupancy factor of 0.5. All hydrogen atoms except for those on the two α-MePy solvent molecules in **1** were put on the calculated positions and were included in the final structure-factor refinement. In the case of **1**, the largest residual electron density (1.75 e/Å^3) in the final Fourier map is close to Mo(1) atom (1.2 Å). All the calculations were carried out on a DELL workstation using the CrystalStructure crystallographic software package (Rigaku and MSC, Ver 3.60, 2004). The crystal data along with the structure refinement parameters for **1** and **2** are summarized in Table 4.

4.2.4. Third-order susceptibility measurement

The third-order susceptibility $\chi^{(3)}$ of **1** or **2** was measured by DFWM with the 35 ps laser pulses (532 nm) generated by a Continuum mode-locked Nd:YAG laser with repetition rate of 10 Hz. The $\chi^{(3)}$ values of the samples were obtained by comparison of the magnitude of the phase conjugate signal with that of the CS_2 reference using Eq. (1) [42a], and the second hyperpolarizability γ was obtained by Eq. (2) [42b]

$$\chi^{(3)}(\text{esu}) = \left(\frac{I}{I_{\text{ref}}}\right)^{1/2}\cdot\frac{d_{\text{ref}}}{d}\cdot\left(\frac{n}{n_{\text{ref}}}\right)^2 \cdot\frac{\alpha\cdot d\cdot\exp(\alpha d/2)}{1-\exp(-\alpha d)}\chi^{(3)}_{\text{ref}}, \quad (1)$$

$$\gamma(\text{esu}) = \frac{\chi^{(3)}}{NL_c}, \quad (2)$$

where I is the intensity of the conjugate signal, n is the linear refractive index, d is the path length, α is the

Table 4
Summary of crystallographic data of $[MoS_4Cu_4(\alpha\text{-MePy})_5Br_2]\cdot 2(\alpha\text{-MePy})_{0.5}$ (**1**) and $[MoS_4Cu_4(\alpha\text{-MePy})_3Br](\mu\text{-Br})\cdot \alpha\text{-MePy}_n$ (**2**)

	1	**2**
Empirical formula	$C_{36}H_{42}Br_2Cu_4MoN_6S_4$	$C_{24}H_{28}Br_2Cu_4MoN_4S_4$
Formula weight	1196.94	1010.68
Crystal system	Triclinic	Orthorhombic
Space group	$P\bar{1}$	$Pca2_1$
a (Å)	11.7717(9)	28.386(2)
b (Å)	13.753(2)	7.6206(5)
c (Å)	16.157(2)	15.1505(12)
α (°)	89.72(3)	
β (°)	74.11(2)	
γ (°)	82.46(2)	
V (Å^3)	2492.7(6)	3277.3(4)
Z	2	4
D_c (g/cm^3)	1.595	2.048
μ (cm^{-1})	37.28	56.48
$2\theta_{max}$ (°)	55.0	55.0
Reflections collected	27346	33021
Unique reflections	10960 (R_{int} = 0.067)	3870 (R_{int} = 0.075)
No. observations ($I > 3.00\,\sigma(I)$)	3489	2720
No. variables	331	240
R[a]	0.070	0.029
R_w[b]	0.081	0.030
GOF[c]	1.090	0.839
Largest residual peaks and holes (e/Å^3)	1.75, −0.94	0.55, −0.68

[a] $R = \sum||F_o|-|F_c||/\sum|F_o|$.
[b] $R_w = \{w\sum(|F_o|-|F_c|)^2/\sum w|F_o|^2\}^{1/2}$.
[c] GOF = $\{\sum w(|F_o|-|F_c|)^2/(M-N)\}^{1/2}$, where M is the number of reflections and N is the number of parameters.

linear absorption coefficient, N is the number density (concentration) of the cluster in the sample and $L_c = [(n^2 + 2)/3]^4$ is the Lorentz field factor correction. The subscript "ref" refers to CS_2 with a value of $\chi^{(3)} = 6.8 \times 10^{-13}$ esu at 532 nm for the 35 ps laser [42c].

Acknowledgements

This work was supported by the NNSF of China (No. 20271036), the NSF of Jiangsu Province (No. BK2004205), the Key Laboratory of Organic Synthesis of Jiangsu Province (No. JSK001), the State Key Laboratory of Organometallic Chemistry of SIOC (No. 04-31), and the Scientific Research Foundation for the Returned Overseas Chinese Scholars, State Education Ministry of China. The authors also thank the reviewers of this paper for their instructive comments.

Appendix A. Supplementary data

Crystallographic data for the structural analyses have been deposited with Cambridge Crystallographic Data Centre, CCDC Nos. 240182 (**1**) and 240183 (**2**). Copies of this information may be obtained free of charge from The Director, CCDC, 12 Union Road, Cambridge, CB2 1E2, UK (fax: +44 1223 336033; email: deposit@ccdc.cam.ac.uk or www: http://www.ccdc.cam.ac.uk). Supplementary data associated with this article can be found, in the online version, at doi:10.1016/j.jorganchem.2004.09.052.

References

[1] (a) A. Müller, E. Diemann, R. Jostes, H. Bögge, Angew. Chem. Int. Ed. 20 (1981) 934;
(b) A. Müller, H. Bögge, U. Schimanski, M. Penk, K. Nieradzik, M. Dartmann, E. Krickemeyer, J. Schimanski, C. Römer, M. Römer, H. Dornfeld, U. Wienböker, W. Hellmann, Monatsh. Chem. 120 (1989) 367.
[2] S. Sarkar, S.B.S. Mishra, Coord. Chem. Rev. 59 (1984) 239.
[3] K.E. Howard, T.B. Rauchfuss, A.L. Rheingold, J. Am. Chem. Soc. 108 (1986) 297.
[4] (a) T. Shibahara, H. Akashi, H. Kuroya, J. Am. Chem. Soc. 110 (1988) 3313;
(b) S. Ogo, T. Suzuki, Y. Ozawa, K. Isobe, Inorg. Chem. 35 (1996) 6093.
[5] (a) Y. Jeannin, F. Sécheresse, S. Bernés, F. Robert, Inorg. Chim. Acta 493 (1992) 198;
(b) J.R. Nicholson, A.C. Flood, C.D. Garner, W. Clegg Soc., J. Chem. Chem. Commun. (1983) 1179.
[6] E.I. Stiefel, D. Coucouvanis, W.E. Newton, Molybdenum Enzymes, Cofactors and Model SystemsACS Symp. Ser., vol. 535, Am. Chem. Soc., Washington, DC, 1993.
[7] X.T. Wu, P.C. Chen, S.W. Du, N.Y. Zhu, J.X. Lu, J. Cluster Sci. 5 (1994) 265.
[8] J.P. Lang, X.Q. Xin, J. Solid State Chem. 108 (1994) 118.
[9] R.H. Holm, Pure Appl. Chem. 67 (1995) 2117.

[10] H.W. Hou, X.Q. Xin, S. Shi, Coord. Chem. Rev. 153 (1996) 25.
[11] D.X. Wu, M.C. Hong, R. Cao, H.Q. Liu, Inorg. Chem. 35 (1996) 1080.
[12] D. Coucouvanis, Adv. Inorg. Chem. 45 (1998) 1.
[13] R.R. Chianelli, T.A. Picoraro, T.R. Halbert, W.H. Pan, E.I. Stiefel, J. Catal. 86 (1984) 226.
[14] T.B. Rauchfuss, Prog. Inorg. Chem. 39 (1991) 259.
[15] M.D. Curtis, Appl. Organomet. Chem. 6 (1992) 429.
[16] R.H. Holm, Adv. Inorg. Chem. 38 (1992) 1.
[17] E.I. Stiefel, K. Matsumoto, Transition Metal Sulfur Chemistry, Biological and Industrial SignificanceAcs. Symp. Ser., vol. 653, Am. Chem. Soc., Washington, DC, 1996.
[18] G.N. George, I.J. Pickering, E.Y. Yu, R.C. Prince, S.A. Bursakov, O.Y. Gavel, I. Moura, J.J.G. Moura, J. Am. Chem. Soc. 122 (2000) 8321.
[19] E.K. Quagraine, R.S. Reid, J. Inorg. Biochem. 85 (2001) 53.
[20] (a) S. Shi, W. Ji, S.H. Tang, J.P. Lang, X.Q. Xin, J. Am. Chem. Soc. 116 (1994) 3615;
(b) S. Shi, W. Ji, J.P. Lang, X.Q. Xin, J. Phys. Chem. 98 (1994) 3570;
(c) S. Shi, W. Ji, W. Xie, S.H. Tang, H.C. Zeng, J.P. Lang, X.Q. Xin, Mater. Chem. Phys. 39 (1995) 298;
(d) J.P. Lang, K. Tatsumi, H. Kawaguchi, J.M. Lu, P. Ge, W. Ji, S. Shi, Inorg. Chem. 35 (1996) 7924;
(e) X.R. Zhu, R.M. Niu, Z.R. Sun, H.P. Zeng, Z.G. Wang, J.P. Lang, Chem. Phys. Lett. 372 (2003) 524;
(f) X.R. Zhu, Z.R. Sun, R.M. Niu, H.P. Zeng, Z.G. Wang, J.P. Lang, Z.Z. Xu, R.X. Li, J. Appl. Phys. 94 (2003) 4772.
[21] C.M. Che, B.H. Xia, J.S. Huang, C.K. Chan, Z.Y. Zhou, K.K. Cheung, Chem. Eur. J. 7 (2001) 3998.
[22] (a) C. Zhang, Y.L. Song, B.M. Fung, Z.L. Xue, X.Q. Xin, Chem. Commun. (2001) 843;
(b) C. Zhang, Y.L. Song, F.E. Kuhn, Y. Xu, X.Q. Xin, H.K. Fun, W.A. Herrmann, Eur. J. Inorg. Chem. (2002) 55;
(c) G.X. Jin, Ph.D. Thesis, Nanjing University, Nanjing, China, 1987;
(d) G.X. Jin, X.Q. Xin, A.B. Dai, J.H. Wu, B.Y. Wang, P.J. Zheng, ZIRAN 10 (1988) 873.
[23] (a) J.G. Li, F.J. Gao, J.P. Lang, X.Q. Xin, M.Q. Chen, Chin. J. Struct. Chem. 11 (1992) 351;
(b) J.P. Lang, W.Y. hou, X.Q. Xin, J.H. Cai, B.S. Kang, K.B. Yu, Polyhedron 12 (1993) 1647;
(c) J.P. Lang, X.Q. Xin, K.B. Yu, J. Coord. Chem. 33 (1994) 99;
(d) M.T. Pope, J.P. Lang, X.Q. Xin, K.B. Yu, Chin. J. Chem. 13 (1995) 40;
(e) Q. Huang, X.T. Wu, T.L. Sheng, Q.M. Wang, Inorg. Chem. 34 (1996) 4931.
[24] H.W. Hou, H.G. Zheng, G.A. How, Y.F. Fan, M.K.M. Low, Z. Yu, W.L. Wang, X.Q. Xin, W. Ji, W.T. Wong, J. Chem. Soc., Dalton Trans. (1999) 2953.
[25] (a) J.P. Lang, K. Tatsumi, Inorg. Chem. 37 (1998) 6308;
(b) H. Yu, Q.F. Xu, Z.R. Sun, S.J. Ji, J.X. Chen, Q. Liu, J.P. Lang, K. Tatsumi, Chem. Commun. (2001) 2614.
[26] (a) J.P. Lang, S.J. Ji, Q.F. Xu, Q. Shen, K. Tatsumi, Coord. Chem. Rev. 241 (2003) 47;
(b) J.P. Lang, Q.F. Xu, Z.N. Chen, B.F. Abrahams, J. Am. Chem. Soc. 125 (2003) 12682;
(c) J.P. Lang, Q.F. Xu, W. Ji, H.I. Elim, K. Tatsumi, Eur. J. Inorg. Chem. (2004) 86.
[27] (a) J.M. Manoli, C. Potvin, F. Sécheresse, S. Marzak, Inorg. Chim. Acta 150 (1988) 257;
(b) F. Sécheresse, S. Bernés, F. Robert, Y. Jeannin, J. Chem. Soc., Dalton Trans. (1991) 2875.
[28] J.P. Lang, H. Kawaguchi, S. Ohnishi, K. Tatsumi, Inorg. Chim. Acta 283 (1998) 136.
[29] (a) J.P. Lang, K. Tatsumi, J. Organomet. Chem 579 (1999) 332;
(b) M. Asplund, S. Jagner, Acta Chem. Scand. A 38 (1984) 135;
(c) M. Asplund, S. Jagner, Acta Chem. Scand. A 38 (1984) 725.
[30] S. Guha, C.C. Frazier, P.L. Porter, K. Kang, S.E. Finberg, Opt. Lett. 14 (1989) 952.
[31] W.J. Blau, H.J. Byrne, D.J. Gardin, A.P. Davey, J. Mater. Chem. 1 (1991) 245.
[32] M. Hosoda, T. Wada, A. Yamada, A.F. Garito, H. Sasabe, Mat. Res. Soc. Symp. Proc. 175 (1990) 89.
[33] M. Hosoda, T. Wada, A. Yamada, A.F. Garito, Jpn. J. Appl. Phys. 30 (1991) L1486.
[34] Y. Wang, L.T. Cheng, J. Phys. Chem. 96 (1992) 1530.
[35] T. Zhai, C.M. Lawson, D.C. Gale, G.M. Gray, Opt. Mater. 4 (1995) 455.
[36] L.K. Myers, C. Langhoff, M.E. Thompson, J. Am. Chem. Soc. 114 (1992) 7560.
[37] D.V.G.L.N. Rao, F.J. Aranda, J.F. Roach, D.E. Remy, Appl. Phys. Lett. 58 (1991) 1241.
[38] J.W. McDonald, G.D. Friesen, L.D. Rosenhein, W.E. Newton, Inorg. Chim. Acta 72 (1983) 205.
[39] P.T. Beurskens, G. Admiraal, G. Beurskens, W.P. Bosman, S. Garcia-Granda, R.O. Gould, J.M.M. Smits, C. Smykalla, PATTY, The DIRDIF Program System, Technical Report of the Crystallography Laboratory, University of Nijmegen, The Netherlands, 1992.
[40] G.M. Sheldrick, SHELXS-97, Program for the Solution of Crystal Structure, University of Goettingen, Germany, 1997.
[41] P.T. Beurskens, G. Admiraal, G. Beurskens, W.P. Bosman, R. de Gelder, R. Israel, J.M.M. Smits, DIRDIF99, The DIRDIF-99 Program System, Technical Report of the Crystallography Laboratory, University of Nijmegen, The Netherlands, 1999.
[42] (a) P.L. Ramazza, S. Ducci, S. Boccaletti, F.T. Arecchi, J. Opt. B 2 (2000) 399;
(b) K. Hasharoni, H. Levanon, S.R. Greenfield, D.J. Gosztola, W.A. Svec, M.R. Wasielewski, J. Am. Chem. Soc. 118 (1996) 10228;
(c) N.P. Xuan, J.L. Ferrier, J. Gazengel, G. Rivoire, Opt. Commun. 51 (1984) 433.